Fluid-Rock Interaction Models: Code Release and Results

Edward W. Bolton, Yale University
   Department of Geology and Geophysics,
   P.O. Box 208109, New Haven, CT, 06520-8109
Email: edward.bolton@yale.edu
Phone: 1-203-432-3149

Adapted from: Poster: V31B-0592
Fall 2006, American Geophysical Union

Abstract

Numerical models our group has developed for understanding the role of kinetic processes during fluid-rock interaction will be released **free** to the public. We will also present results that highlight the importance of kinetic processes. The author is preparing manuals describing the numerical methods used, as well as "how-to" guides for using the models. The release will include input files, full in-line code documentation of the FORTRAN source code, and instructions for use of model output for visualization and analysis. The aqueous phase (weathering) and supercritical (mixed-volatile metamorphic) fluid flow and reaction models for porous media will be released separately. These codes will be useful as teaching and research tools. The codes may be run on current generation personal computers. Although other codes are available for attacking some of the problems we address, unique aspects of our codes include sub-grid-scale grain models to track grain size changes, as well as dynamic porosity and permeability. Also, as the flow field can change significantly over the course of the simulation, efficient solution methods have been developed for the repeated solution of Poisson-type equations that arise from Darcy's law. These include sparse-matrix methods as well as the even more efficient spectral-transform technique. Results will be presented for kinetic control of reaction pathways and for heterogeneous media. Codes and documentation for modeling intra-grain diffusion of trace elements and isotopes, and exchange of these between grains and moving fluids will also be released. The unique aspect of this model is that it includes concurrent diffusion and grain growth or dissolution for multiple mineral types (low-diffusion regridding has been developed to deal with the moving-boundary problem at the fluid/mineral interface). Results for finite diffusion rates will be compared to batch and fractional melting models. Additional code and documentation will be released for modeling diffusion and consumption of oxygen by ancient organic matter and pyrite in an eroding shale soil, as relevant for understanding an important boundary condition for the long-term evolution of Earth's atmosphere. Results indicate that ancient organic matter is normally oxidized before eroding except for rapid erosion rates. The source codes can be readily modified for use in other reactive-transport models or for individual use.

Adapted from Bolton (2006) poster V31B-0592, Fall AGU

Four code families will be released related to fluid-rock interaction

KINFLOW - mineral reactions and nonisothermal aqueous phase solute transport in 2D

META-KINFLOW - mineral reactions and nonisothermal supercritical H_2O-CO_2 mixture transport in 2D

DIG - isotope or trace element diffusion in mineral grains during recrystallization with fluid flow interactions

OMPYR - oxygen diffusion in eroding soils and oxidation reactions of ancient organic matter and pyrite

KINFLOW: Aqueous phase reactive transport model in porous media with kinetic control of mineral reactions

MAIN FEATURES:

- **Non-isothermal flow in porous media**
- **Dynamic heterogeneous porosity and permeability**
- **Sub-grid-scale grain models for minerals** (see figure below)
- **Thermal evolution with reactive heating**
- **Mineral dissolutions and precipitation via experimental kinetics**
- **Speciation reactions in solution in equilibrium** (except for redox reactions in future species sets)
- **Evolving flow via Darcy's law with buoyancy effects solved by:**
    - **Spectral transform technique, or**
    - **Sparse matrix solution**
- **Simple system: Na-Al-Si-O-H**
- **Minerals:** albite, quartz, gibbsite, paragonite, and kaolinite
- **10 aqueous Species**
- **Temperature dependent speciation via EQ3/6,** from 0-300°C
- **Dozens more minerals and species are being added to the code**
- **Advection schemes:** various choices: upwinding, Leonard's third-order scheme, …
- Boundary conditions: various: no flux, imposed flux, imposed values

See KINFLOW results in Figs. 1&2.

Grain models
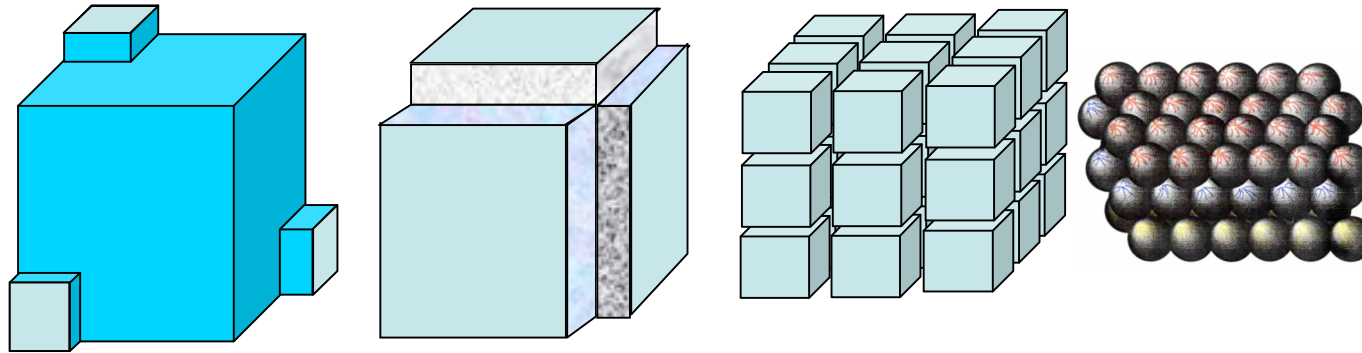
Grain contact areas are the light end caps

Grain model parameters for fluid flow and mineral reaction kinetics: Grain volumes, spacing, porosity, surface areas, fluid gap spacing, and the permeability - shown here for **cubic grain model**

- Grain volume fraction for mineral m. $\phi_m = \overline{N}_m d_m^3$

- Nucleation density and grain spacing $\overline{N}_m = 1 / l_m^3$

- Porosity for the fluid saturated case $\phi = 1 - \sum_{m=1}^{N_{min}} \phi_m$

- Surface areas compared to fluid volume: $\dfrac{A_m}{V_f} = \dfrac{1}{\phi}\left(6\overline{N}_m d_m^2\right)$

- Fluid gap spacing estimate $\delta = \dfrac{2 \cdot \text{fluid volume}}{\text{total surface area}} = \dfrac{\phi}{\left(3\sum_{m=1}^{N_{min}} \overline{N}_m d_m^2\right)}$

- Permeability (m^2) $k = (\phi\delta^2)/36$

Adapted from Bolton (2006) poster V31B-0592, Fall AGU

Fast solutions of Poisson equations

Darcy's law coupled with mass conservation must be solved repeatedly when porosities and permeabilities change.

This can be due to mineral dissolution and precipitation, or due to compaction, buoyancy effects or reactive production of fluids (e.g., via decarbonation reactions). Sparse-matrix and spectral-transform techniques have both been found to be more efficient than conjugate gradient methods, and have been adapted to a variety of boundary conditions. For the mixed-volatile code, an anelastic type of approximation has been used.

SPARSE-MATRIX METHOD
- Eisenstat et al., (1977a,b)
- Very versatile for boundary conditions

SPECTRAL-TRANSFORM METHOD
- Based on Christensen and Harder (1991)
- Quite versatile for boundary conditions

Both with
- Dynamic heterogeneous porosity and permeability
- Buoyancy driven flow
- Compaction driven flow
- Various boundary conditions
    - no-flux
    - constant flux
    - constant pressure
        (variable flux dependent on spatial variations of permeability).

Log-transforms for high permeability contrasts: These are being tested and will be released.

- **Solute concentration c_i (mol/m³): multiple species**

$$\frac{\partial}{\partial t}(\phi c_i) + \nabla \bullet (c_i \mathbf{q}) = R_i' - \nabla \bullet (\phi \mathbf{j}'_i)$$

| Advection | Reactions affecting c_i | | Diffusive and Dispersive fluxes |

Local time rate of change
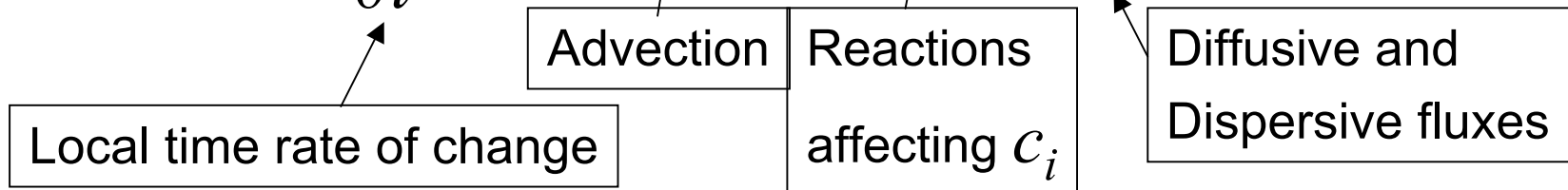
- **Solution species affected by kinetic and equilibrium relations**

- **For kinetic control of mineral i dissolution/precipitation:**

$$\frac{R_i}{\phi} = \frac{\text{Mineral Area}_i}{\text{Volume}_{fluid}} * k_o * \exp\left(-\frac{E_a}{RT}\right) * \prod_j a_j^{n_j} f(\Delta G)$$

Dependence on deviation from equilibrium

Rate Constant

Temperature dependence

Catalysts or Inhibitors
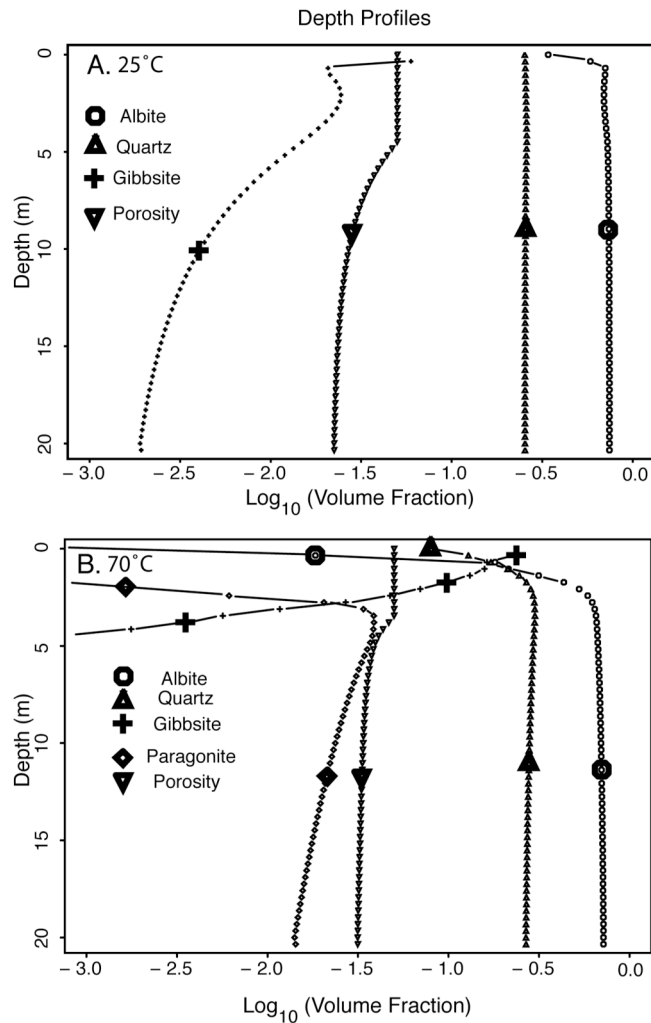
Depth Profiles

Figure 1. Results of KINFLOW for present verses Archean Hot House weathering of an albite-quartz matrix (Bolton and Rob Rye, 2006, in preparation).
Depth profiles of minerals for two different temperatures (A: 25°C, B: 70°C) after 60,000 years of water infiltration into a matrix initially composed of 25% quartz, and 75 % albite, in a Na, Si, Al, O, H system. Initial porosity was 2% and infiltration was about 1 cubic m/yr per m^2 land surface. The grain spacing was 1 mm for quartz and albite and 0.4 mm for all other minerals. The order of abundance of minerals at the surface for 25°C (albite, quartz, gibbsite) is reversed for the 70°C run. The simulation also includes kaolinite as a secondary mineral, but only trace amounts exist. Ten aqueous species are included in the calculation, as well as downward solute transport, and some compaction. All mineral reactions are based on kinetic control.

Effect of permeability heterogeneity on flow velocity and extent of chemical disequilibrium

A.

Gray scale: Darcy flux ($m^3/m^2/yr$)

B.

Figure 2.

A. Quasi-steady flow through a heterogeneous porous medium. Fluid injected at z=0, with flow parallel to the dashed curves, and Darcy velocity in gray scale with an average magnitude of 9.4 $m^3/m^2/yr$: a value between typical fluxes in soils and typical column kinetic dissolution experiments (e.g., White and Brantley, 2003, used a value of 175 $m^3/m^2/yr$ in their experiment). Solid curves are the silicic acid concentration normalized as $(c - c_{eq})/c_{eq}$ to indicate the deviation from the equilibrium value c_{eq}. Initial conditions: 24.5 vol. % quartz in an otherwise inert matrix. porosity=0.02, T=25 $^{\circ}$C, $\log_{10}$(permeability (m^2)): (min,mean,max)=(-14.5,-13.1,-12). **Faster flow favors greater deviation from equilibrium**.

B. Concentration along vertical cuts of part A, at each x location of the grid. **The considerable variation observed increases with stronger permeability heterogeneity used in other simulations.** Effective rate constant from average solute effluent would not match actual rate constant used.

Adapted from Bolton (2006) poster V31B-0592, Fall AGU

META-KINLFOW: Two-dimensional metamorphic flow / reaction model with overall reactions in supercritical CO_2-H_2O fluids

Thermodynamic database for Dolomite, Quartz, Talc, Calcite, Tremolite, Diopside, Forsterite, Wollastonite (<u>CMS system</u>, Ca, Mg, Si, C, O, H) via Berman + Kerrick & Jacobs CO_2-H_2O equation of state and fugacity. Kinetic control derived from experiments

In addition to thermodynamic and kinetic aspects:

Temperature - heat release from reactions and "pluton"

Fluid flow - gas release or consumption by reactions
- buoyancy effects
- binary supercritical fluid
- barycentric (mass averaged) velocity frame
- full dispersion in 2D

Fully **dynamic** grain size, porosity, **permeability**, via grain models shown above.
Compaction in zones of large reactive solid volume loss
via Balashov & Yardley (1998), Zhang et al. (1994).
Finite difference method with spectral transform or sparse matrix method for flow.
Anelastic approximation for fluid mass (filter out sound waves)
Pressure gradient - hydrostatic basic state

Define the fluid velocity **v** to be the mass average of the component velocities for the binary supercritical fluid (CO_2-H_2O).

- Fluid component velocities : $\mathbf{u}_i$
- Mass fractions : ω_i for each component
- Number of fluid components : N_f

$$\mathbf{v} = \sum_{i=1}^{N_f} \omega_i \mathbf{u}_i$$
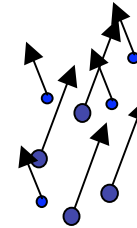
$\mathbf{q} = \phi\, \mathbf{v}$ Relates Darcy and pore velocities via porosity

$$\mathbf{q} = \left(\frac{\partial U}{\partial x} - \frac{\partial \psi}{\partial z}, 0, \frac{\partial U}{\partial z} - \frac{\partial \psi}{\partial x} \right)$$ Darcy flux decomposition

into velocity potential and stream function parts

$\nabla^2 U = \Gamma$ (fluid sources, net advection, or compaction)

$$\gamma \nabla^2 \psi + \frac{\partial \gamma}{\partial z}\left(\frac{\partial \psi}{\partial z} - \frac{\partial U}{\partial x} \right) + \frac{\partial \gamma}{\partial x}\left(\frac{\partial \psi}{\partial x} + \frac{\partial U}{\partial z} \right) = -g\frac{\partial \rho_F}{\partial x}$$

where $\gamma = \dfrac{\mu}{k}$

Reactions 1-5 meet at lowest T isobaric univariant point: IIP#1

1) $3 \text{ Dol} + 4 \text{ Qtz} + H_2O \quad = \text{ Tlc} + 3 \text{ Cal } + 3 \text{ CO}_2$

2) $5 \text{ Tlc } + 6 \text{ Cal } + 4 \text{ Qtz} = 3 \text{ Tr } + 6 \text{ CO}_2 + 2 \text{ H}_2O$

3) $2 \text{ Tlc } + 3 \text{ Cal} \qquad\quad = \text{ Tr } + \text{ Dol } + \text{ CO}_2 + H_2O$

4) $5 \text{ Dol} + 8 \text{ Qtz } + H_2O \quad = \text{ Tr } + 3 \text{ Cal } + 7 \text{ CO}_2$

5) $\text{Tlc } + 2 \text{ Dol } + 4 \text{ Qtz} \quad = \text{ Tr } + 4 \text{ CO}_2$

15 reactions included in the model
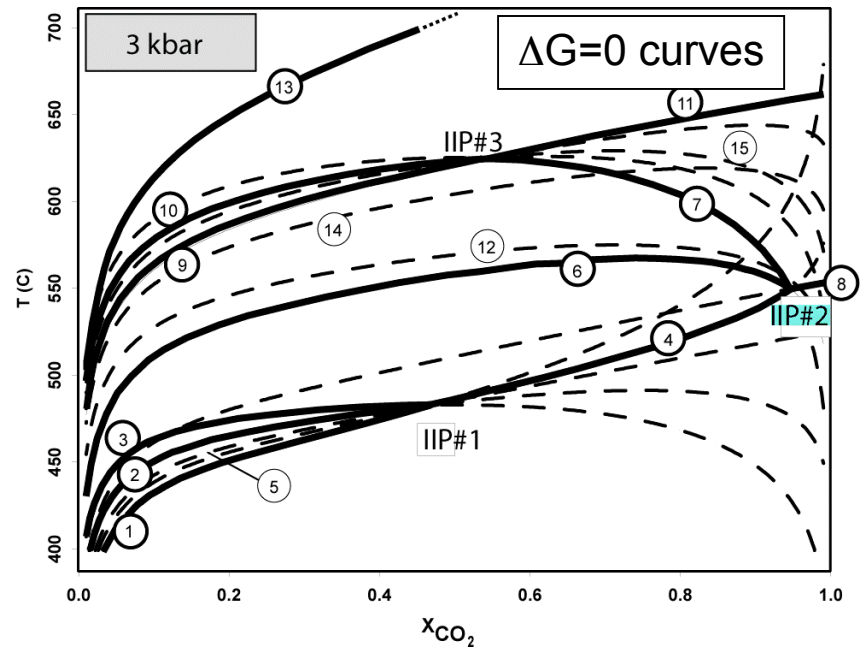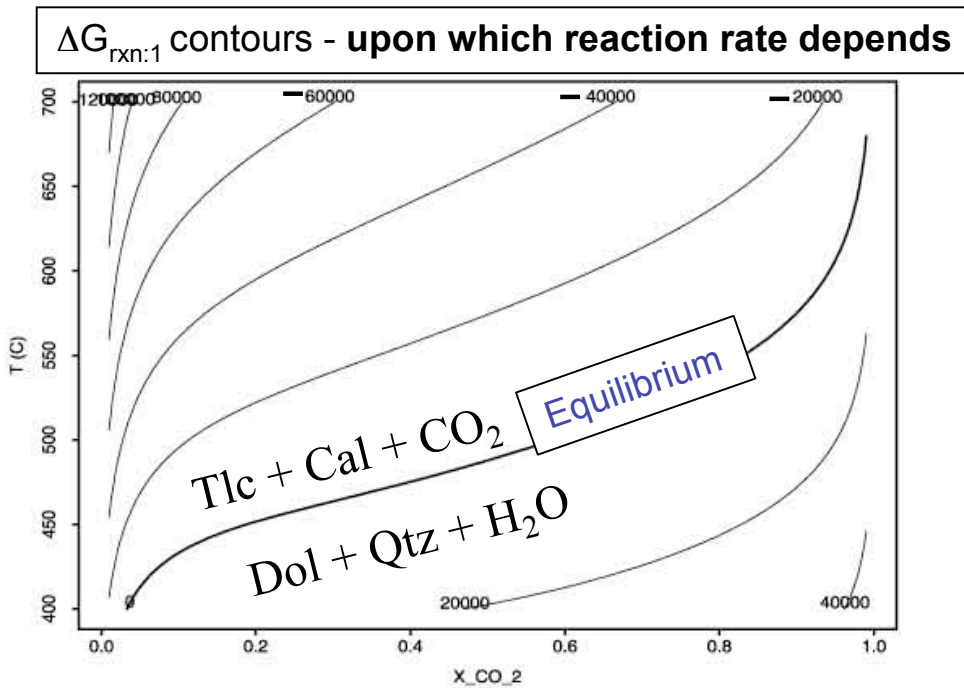
$\Delta G_{rxn:1}$ contours - **upon which reaction rate depends**

Equilibrium

$Tlc + Cal + CO_2$

$Dol + Qtz + H_2O$

3 kbar

$\Delta G=0$ curves

IIP#3

IIP#2

IIP#1

Luttge, Bolton and Rye (2004)

Adapted from Bolton (2006) poster V31B-0592, Fall AGU

Constant heating from Luttge, Bolton, and Rye (2004)

Reaction paths need not follow univariant curves,
nor pass through invariant points.
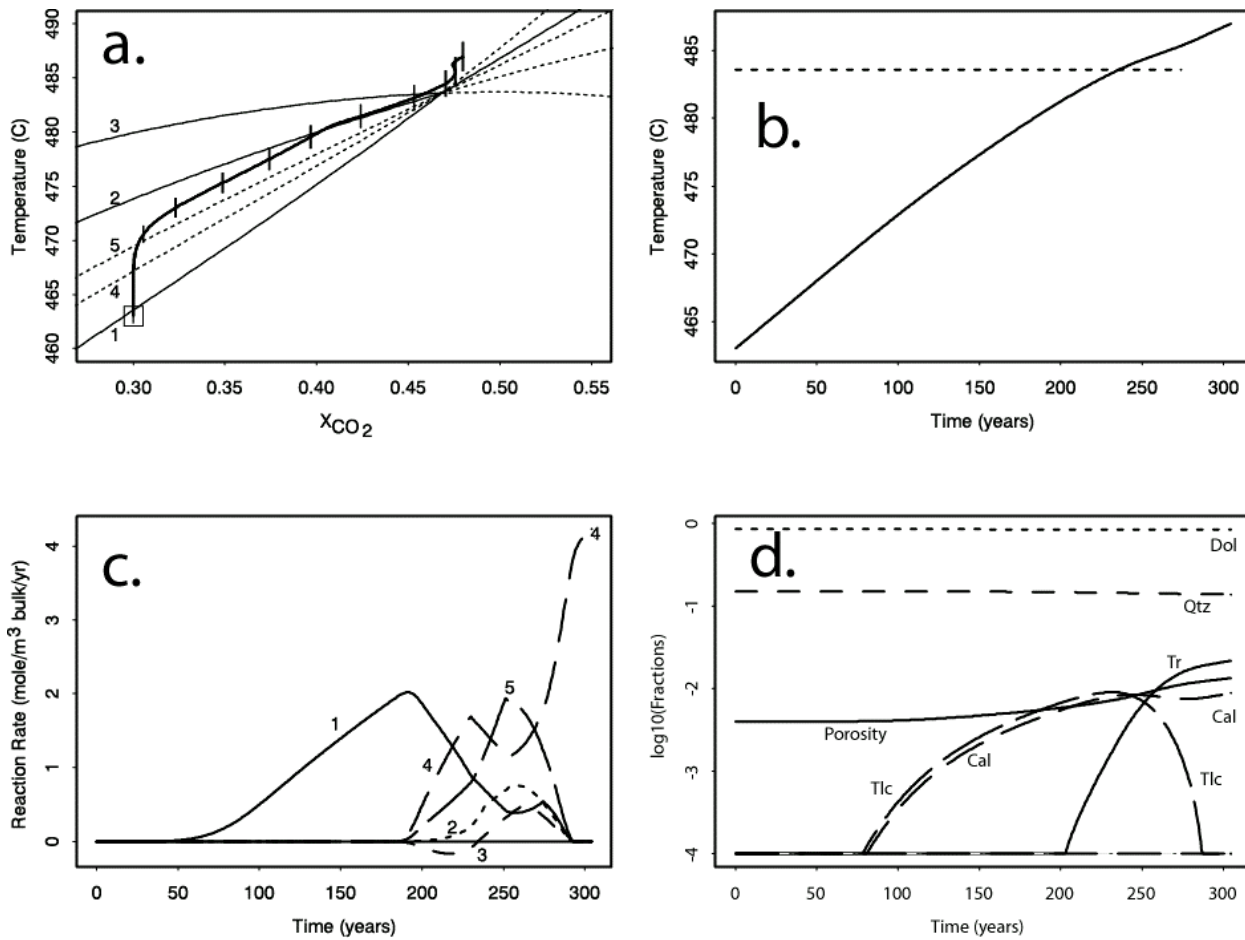
Contact metamorphism model: at several domain locations from Bolton, Luttge, Rye, and Ague (2006, in prep.)
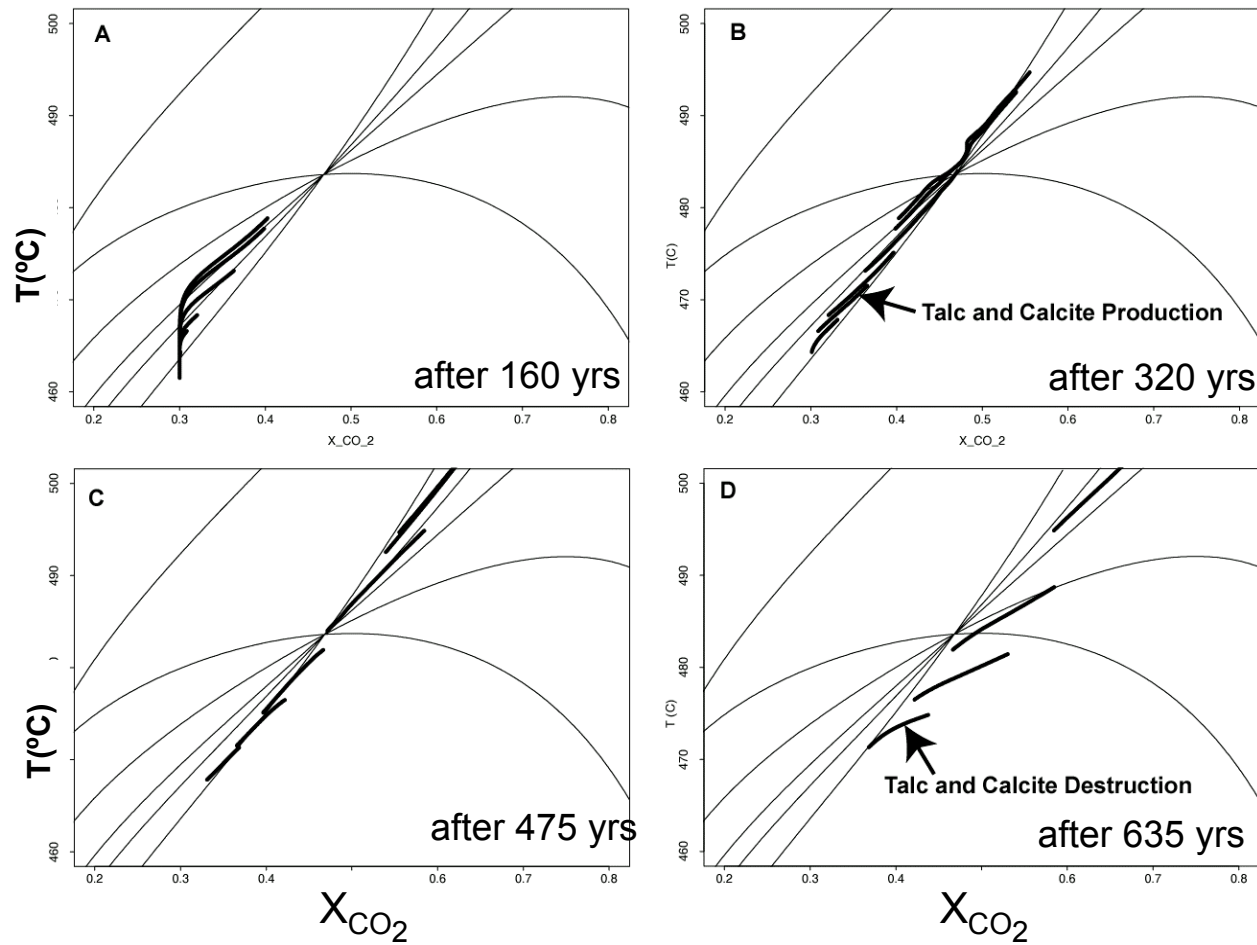
Talc and calcite destruction during prograde heating would not occur via an equilibrium based model.

Contact Metamorphism Model: Note the dramatic influence of grain size.

0.1°C/yr heating rate of lower left boundary. Bolton, Luttge, Rye, Ague (2006, in prep.)

Small grains →

Low perm, high SA

A and B, after 800 yrs, grain spacing 0.4 mm.

Reaction driven flow

Max pore vel = 0.75 m/yr

(perm=permeability)
(SA=mineral surface area)

Large grains →

High perm, low SA

C and D, after 320 yrs. grain spacing 4 mm.

Buoyancy driven flow

Max pore vel = 4 m/yr

Figure 3.

A: velocities with color X_{CO_2}
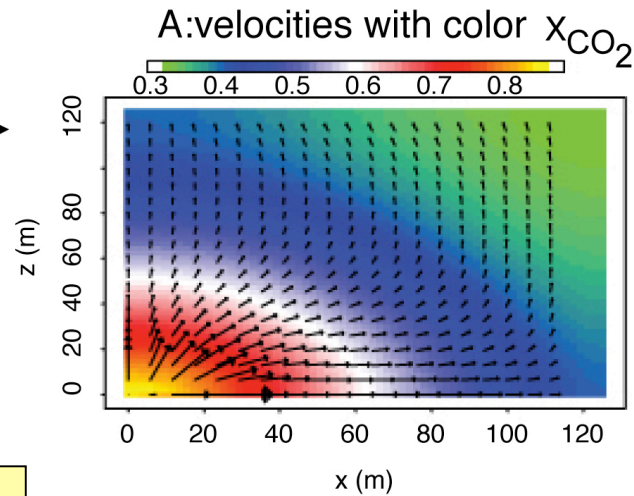
B: $\Delta G=0$ curves + final X,T pairs in domain

C: velocities with color X_{CO_2}
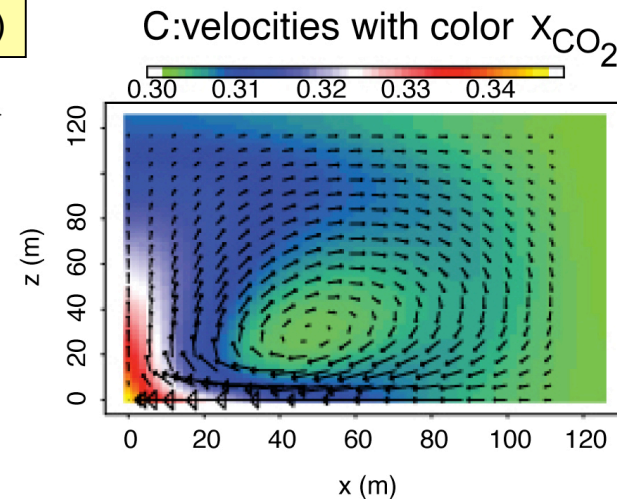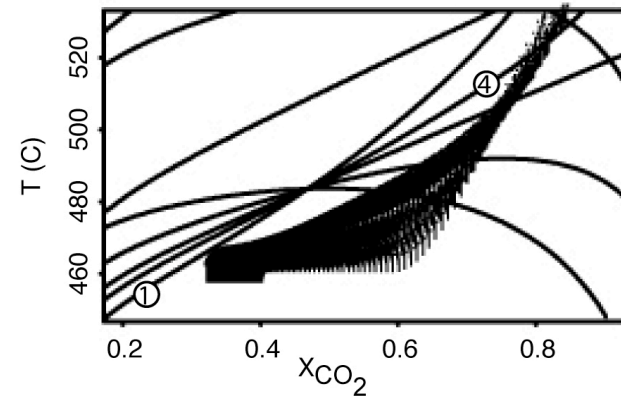
D: $\Delta G=0$ curves + final X,T pairs in domain
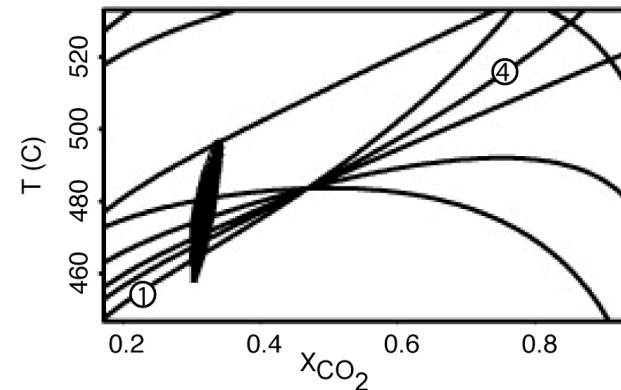
A and C: X_{CO2} and flow (actual velocities for part C are much greater than in A).

B and D: ending T-X_{CO2} pairs for each point (x-z pairs).
rxns 1:Dol+Qtz+H_2O↔Tlc+Cal+CO_2
4:Dol+Qtz+H_2O↔Tr+Cal+CO_2

DIG - <u>D</u>iffusion <u>I</u>n <u>G</u>rains: simultaneous with dissolution and precipitation

MAIN FEATURES:
- **Solve for intragrain diffusion of isotopes (ISO) or trace elements (TE)**
- **Open system with extraction or 1D flow through for fluids**
- **Spherical grains that grow or dissolve**
- **Simultaneous calculation of fluid composition for ISO or TE**
- **Grain size changes dump or extract ISO or TE to/from fluid.**
- **Diffusion exchange between grains and fluid**
- **Comparisons to batch melting or partial melting models**
- **TE code set up for tens of TE**
- **Incorporates data for diffusion in minerals**
- **Fluid/mineral partitioning in equilibrium only at mineral surface**

Diffusion of species j in spherical grains of mineral m of radius a_m in terms of moles/volume c_j

$$\frac{\partial c_j^m}{\partial t} = D_j^m \nabla^2 c_j^m \quad \text{for } 0 \le r \le a_m$$

■ Partition or distribution coefficients if in equilibrium <u>at</u> mineral <u>surfaces</u>, with F for fluid (melt, aqueous, gas),

$$c_j^m = K_j^m c_j^F \quad \text{for } r = a_m$$

■ Both K and D are temperature dependent
   ■ K for isotopes adapted from the α's
■ Dissolution and precipitation complicates the surface boundary condition. Kinetic surface delay easily accommodated by simple generalization of the above.

■ This project is in preparation with Sumit Chakraborty (Bochum, Germany).

Adapted from Bolton (2006) poster V31B-0592, Fall AGU

Exchange of isotopes or elements at mineral / fluid surfaces

$$R_j^m = \overline{N}_m \left\{ -4\pi a_m^2 \left[D_j^m \frac{\partial c_j^m}{\partial r} \Big|_s + \frac{\partial a_j}{\partial t} \left\{ \begin{array}{ll} \overline{c}_j^m \Big|_s & \text{for dissolution of m} \\ K_j^m c_j^F & \text{for precipitation} \end{array} \right\} \right] \right\}$$

Diffusive exchange,
as cores of minerals
not in equilibrium
with rims.

Peel off for dissolution, or
precipitation at equilibrium partitioning

Exchange of isotopes or elements coupled with fluid flow

$$\frac{\partial c_j^F}{\partial t} = \frac{1}{\phi} \left[-c_j^F \frac{\partial \phi}{\partial t} - \nabla \bullet (\mathbf{q} c_j^F) - \nabla \bullet (\phi \mathbf{D}^* \bullet \nabla c_j^F) + \sum_{m=1}^{N_{min}} R_j^m \right]$$

porosity   advection   dispersion+diffusion   reactions
correction

Within mineral grains some regridding is done to account for moving boundary problem

Regridding

● Maintain small enough Δr's near rim for accuracy
(but not too small for numerical stability)

● Existing nodes should not just be stretched
(leading to excessive numerical diffusion)

Precipitation   ⊙ = new node   ✕ = remove

← interior   r = a (surface)

Do not change
radial positions
upon regridding

Time

r = 0   *coarse grid*   *fine grid*   r = a

Dissolution   (Many more grid points are used
than are shown in these schematics)

r = 0   r = a

Time

✕ Courant
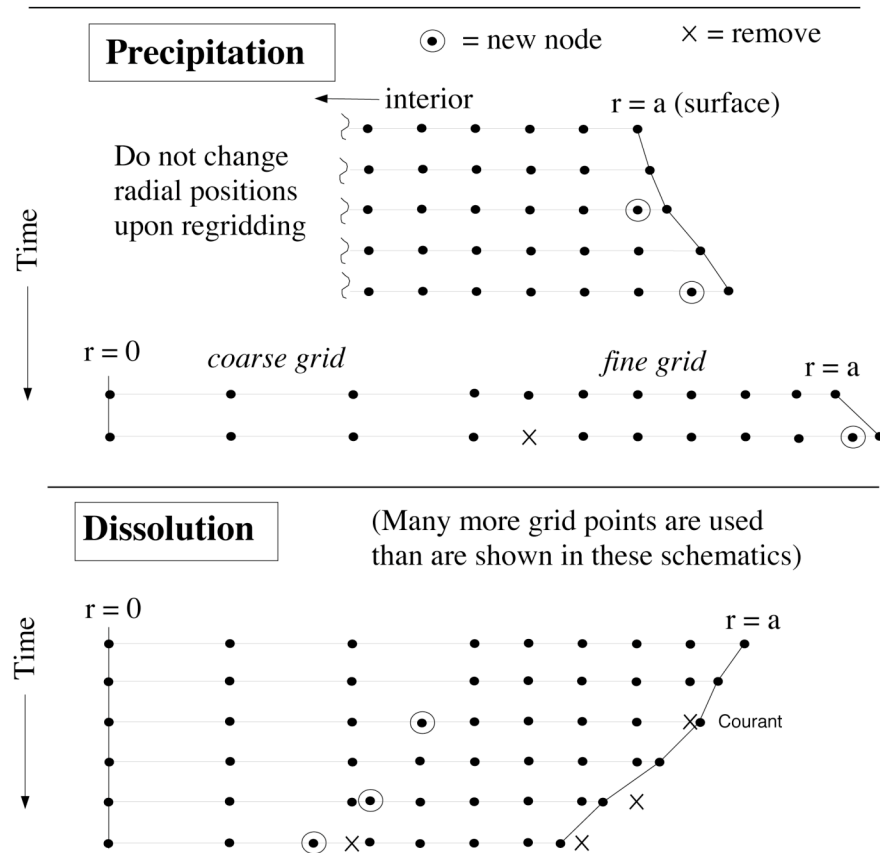
Figure 4. Sample calculation of isotopic diffusion in calcite grains at 500°C during Ostwald ripening compared to experiment. The volume fraction of small and large grains are equal at the start, then the small grains dissolve as the large grains grow. (a) fractional isotope exchange F evolution of model (curve) and Chai (1975) experiment □. Early in the experiment isotopic exchange is dominated by dissolution of the small grains and reprecipitation on the larger grains. At later times, exchange is dominated by diffusion in the resulting larger grains. After very long times, profiles in the grains become flat, and F evolves to the equilibrium value of 1. Here, $F = (\alpha_t - \alpha_i)/(\alpha_{eqm} - \alpha_{init})$, with $\alpha = R_{min}/R_{fluid}$, and $R = [^{18}O]/[^{16}O]$ a concentration ratio; subscripts t: time evolving quantity; i: initial value; eqm: equilibrium value; init: initial value; min: mineral value (cf., Northrop and Clayton, 1966). Last data point with arrow is for t = 672 hrs. (b) profiles in the small grains at various times (S=start, E=end). (c) similar profiles for large grains (initially 12.5 μm radii), growing to about 16 μm. Note slight broadening of diffusion front with reverse zonation. Parts (d-i) represent: evolution of indicated quantities with time.

Adapted from Bolton (2006) poster V31B-0592, Fall AGU

Modeling grain-scale processes:
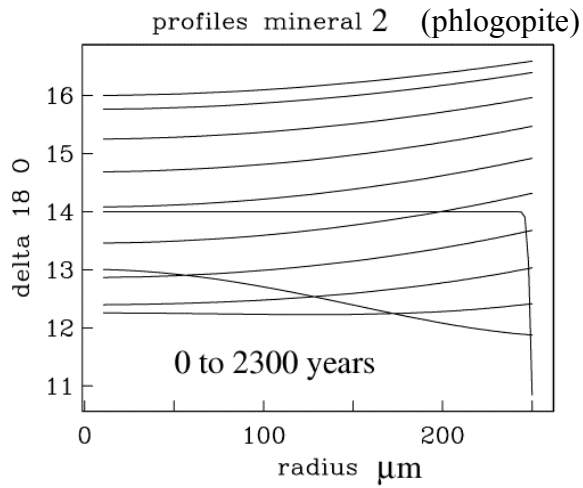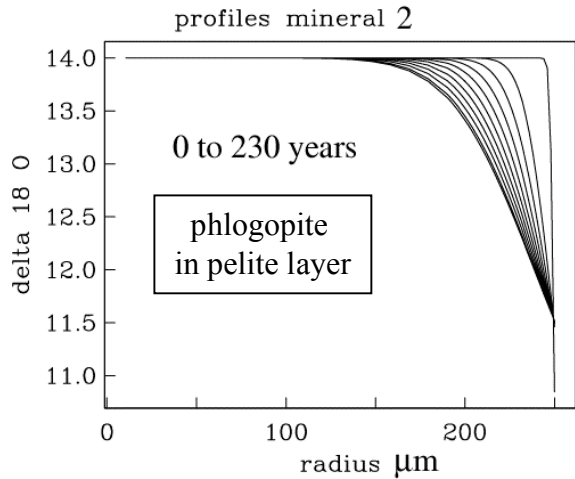a 1D example.

Growing mineral C

Growing mineral D

Dissolving mineral A

Dissolving mineral B
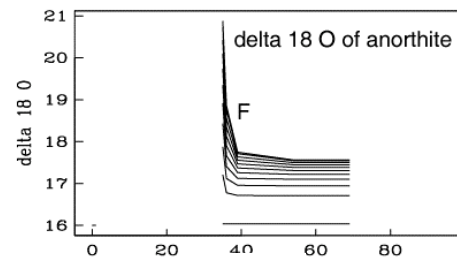(large size fraction)

Dissolving mineral B
(small size fraction)

Fluid Flow Out

Least Reacted
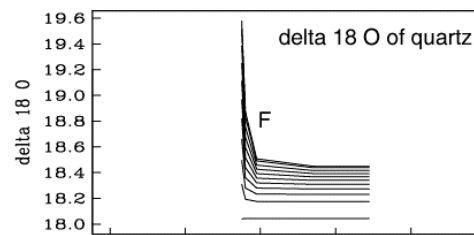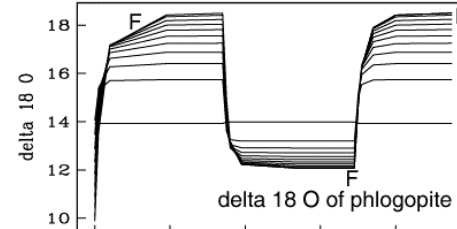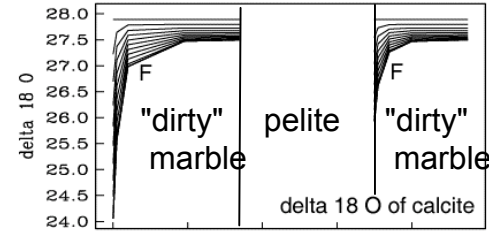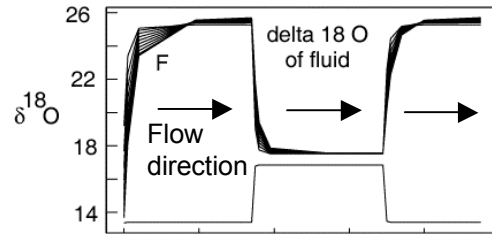
Most Reacted

Fluid Flow Inlet
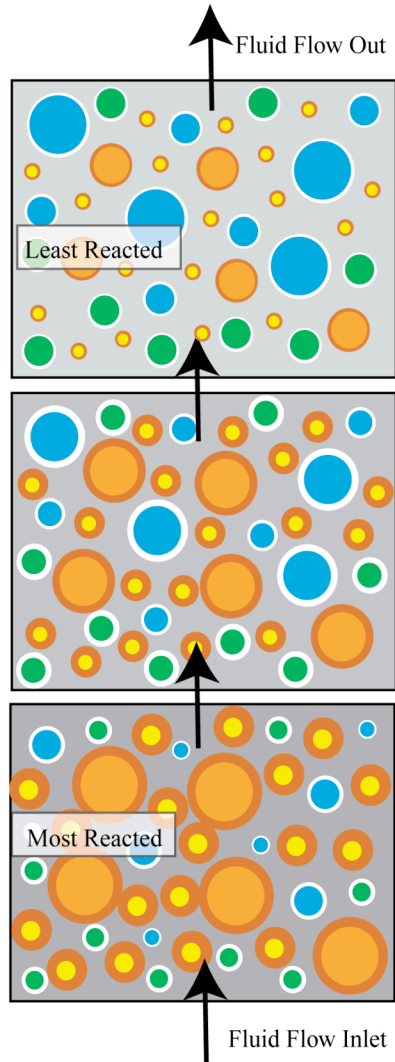
Fluid is injected at the bottom into a
system composed of mineral grains.
The input fluid is far from equilibrium
(darker background shading) with
saturation state favoring the growth
of C and D and dissolution of A and B.
Less mineral size changes occurred
at the top than the bottom.
Cool-colored grains are dissolving,
while warm-colored grains are
precipitating. Each box represents
an REV (representative elementary
volume), along a one-dimensional
flow path. Each REV contains a
specified nucleation density of each
grain type. Within a given mineral
type and size fraction, all the grains
within an REV behave the same.
Mineral growth and dissolution is to be
calculated by kinetic control. Isotope
and trace element diffusion are calculated
for each *type* of grain using a 1D,
spherically symmetric diffusion equation
with a moving boundary at the surface.
(Here, a grain type is a mineral type in
an initial size fraction: five types are
represented here, with mineral B in
two size fractions. Calculations are
performed for each grain type, but
not each individual grain!).
The bottom cell (near the inlet) has
undergone the most dissolution of
A and B and the most growth of C and D.

Example of Isotopic Model
- code capable for diffusion
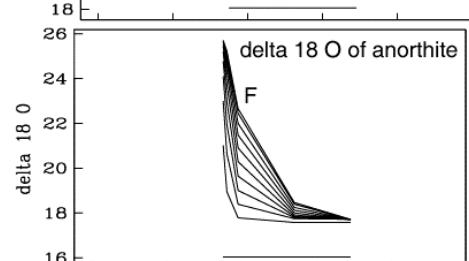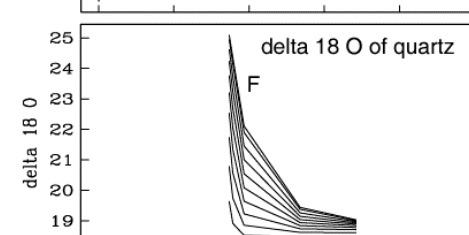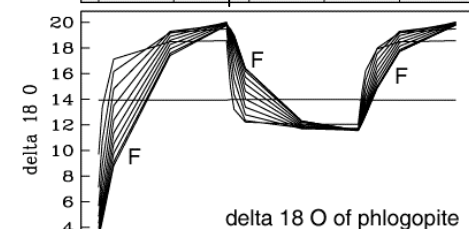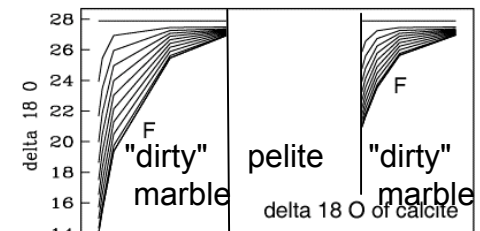 with moving grain boundaries
Fluid injected into 3 rock layers

Diffusion in minerals at 600 °C

profiles mineral 2

0 to 230 years

phlogopite
in pelite layer

profiles mineral 2   (phlogopite)

0 to 2300 years

Adapted from Bolton (2006) poster V31B-0592, Fall AGU
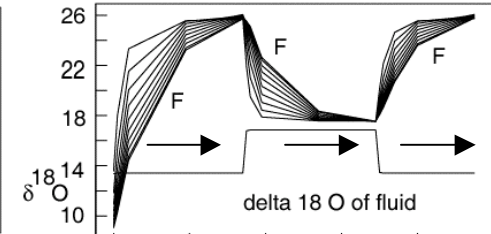
Isotopic Evolution of Fluid and Minerals
Fluid flow from left to right through 3 distinct lithologies

time from start to 230 years   time from start to 2300 years

delta 18 O of fluid

Flow
direction

"dirty" marble   pelite   "dirty" marble

delta 18 O of calcite

delta 18 O of phlogopite

delta 18 O of quartz

delta 18 O of anorthite

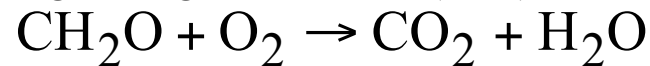"F" for Final profile   x (m)

x (m)

OMPYR: A Model for <u>O</u>rganic <u>M</u>atter and <u>Py</u>rite Oxidation, via gaseous diffusion, reaction, and surface erosion. cf. Bolton, Berner, and Petsch (2006)

Long-term atmospheric oxygen evolution;
Burial and oxidation of organic matter
Is there an erosion rate link?
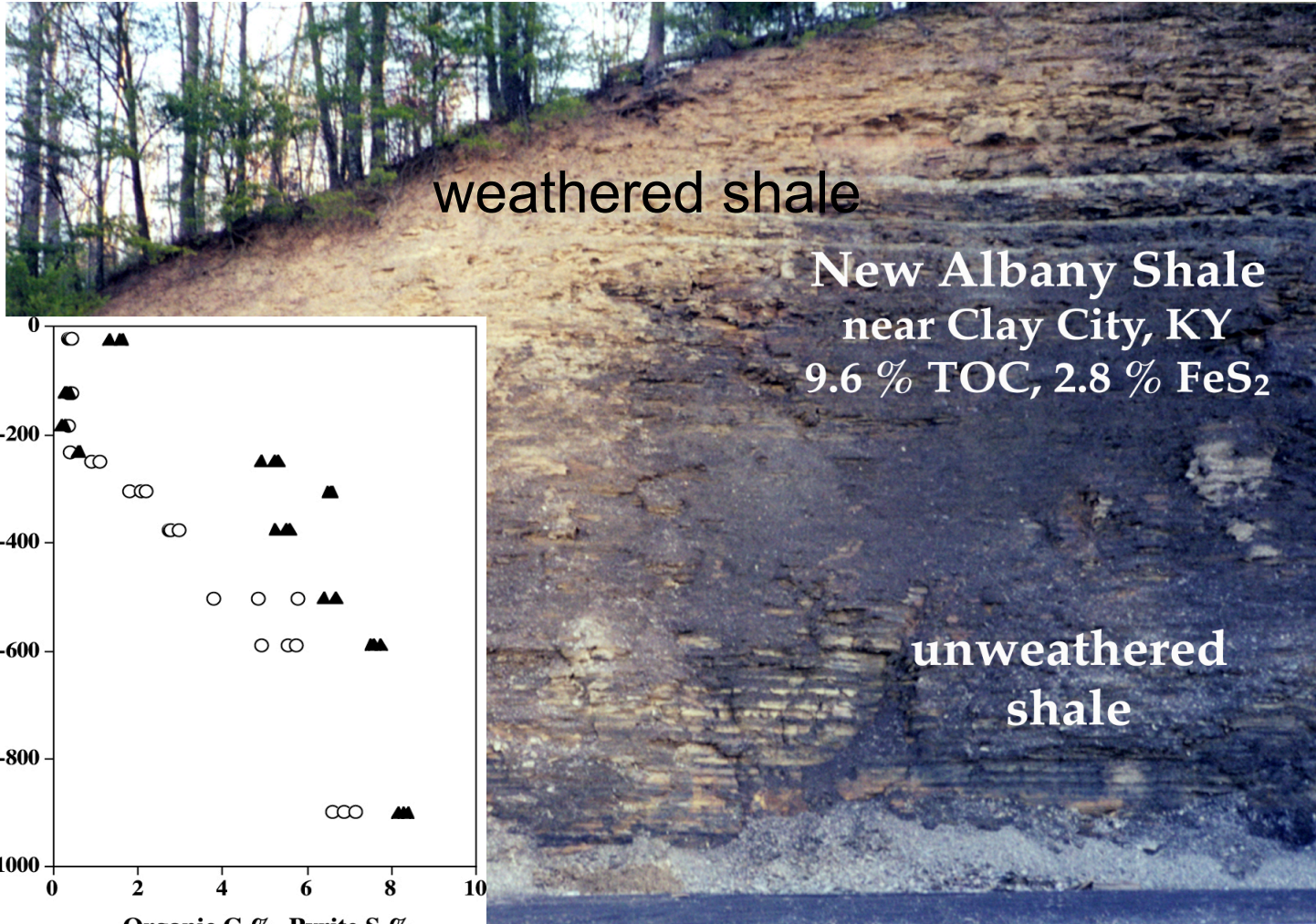
■Weathering of organic matter (OM) consumes oxygen

$$CH_2O + O_2 \rightarrow CO_2 + H_2O$$

■Also, pyrite oxidation consumes oxygen and may play a role in controlling pH, faster reactions

$$4FeS_2 + 15O_2 + 8H_2O \rightarrow 2Fe_2O_3 + 8H_2SO_4$$
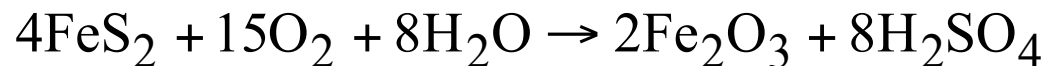
■Understanding of black shale weathering
■Address the debate:
Lasaga and Ohmoto (2002); Holland (2003); Ohmoto (2003)

weathered shale

New Albany Shale
near Clay City, KY
9.6 % TOC, 2.8 % FeS_2

unweathered shale

Depth (cm)

Organic C %, Pyrite S %

Data from Wildman et al., (2004)
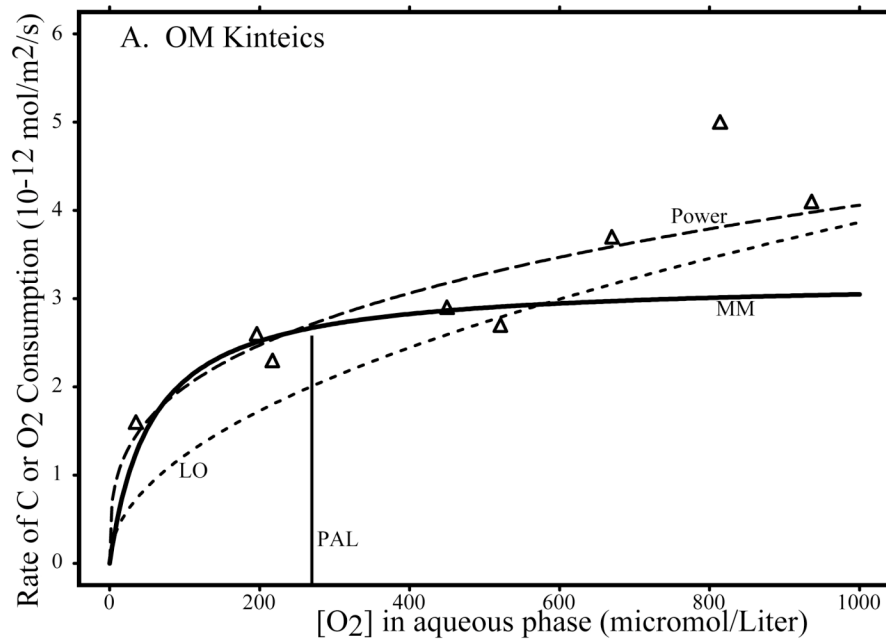
Formulation of Bolton, Berner, and Petsch, (2006)

$$\frac{\partial a}{\partial t} = D_s \frac{\partial^2 a}{\partial x^2} - \sum_i \frac{R_{max}^{*,i} a g_i}{K_m^i + a}\left(\frac{1}{\phi s}\right)\nu_i$$

$$\frac{\partial g_i}{\partial t} = -\omega \frac{\partial g_i}{\partial x} - \frac{R_{max}^{*,i} a g_i}{K_m^i + a} \quad \text{for each} \quad i$$

- a for oxygen concentration in gas + **diffusion**, **reaction**
- g_i for concentration of oxidizing matter +**erosion**, **reaction**
  - e.g., OM, pyrite, _or various grain sizes !_

ω is uplift/erosion rate, Equations for g_i in surface frame. porosity (ϕ) and air saturation (s), stoichiometry (ν), D_s effective diffusion coefficient with porosity and tortuosity dependence: $D_s = T* D_{air}$ with $T* = b\,\phi^{n*}$, $R*$ includes experimentally measured kinetics, $A/V \sim 1/d_i$, and **Henry's law** effects for oxygen fractionation between gas and **fluid films**.

Reaction term shown is for Michaelis-Menten kinetics.
The code also allows choice of power-law kinetics.

A. OM Kineitcs

Rate of C or O$_2$ Consumption (10^{-12} mol/m^2/s)

Power

MM

LO

PAL

[O$_2$] in aqueous phase (micromol/Liter)

B. Pyrite Kinetics

Ⓖ = Biotic rates

Log$_{10}$(Rate of Pyrite Oxidation (mol/m^2/s))

Abiotic rates
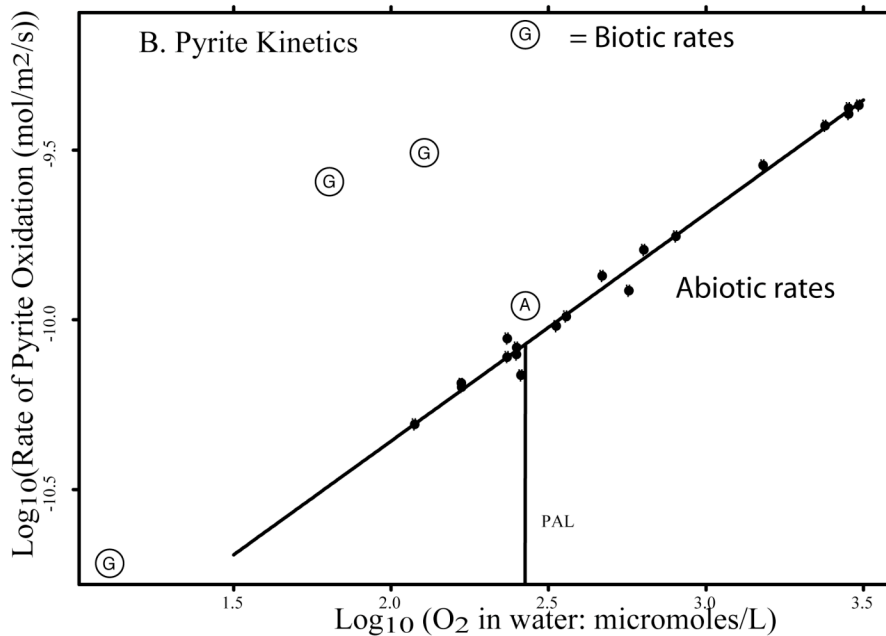
PAL

Log$_{10}$ (O$_2$ in water: micromoles/L)

From Bolton, Berner, and Petsch, (2006)

Coal oxidation kinetics from
Chang and Berner (1999).

Power-law and Michaelis-Menton fits
from Bolton et al., (2006).

LO is the fit used by
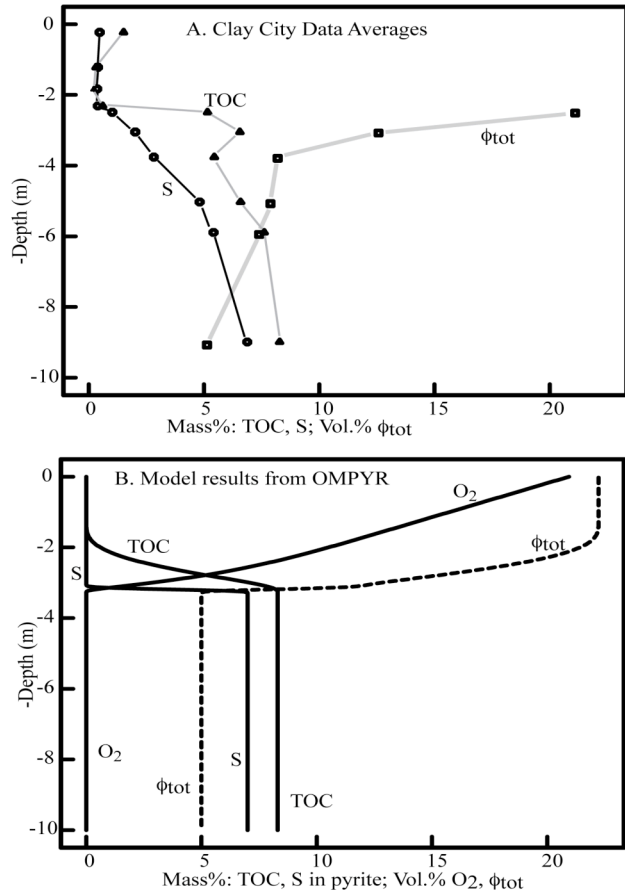Lasaga and Ohmoto (2002).

Pyrite oxidation kinetics from
Smith and Shumate (1970) [closed circles]
and Gleisner et al., (2004) [open circles]

Power-law fit from Bolton et al., (2006)
for abiotic rates.

PAL represents the dissolved oxygen in
equilibrium with present atmospheric O$_2$
level.

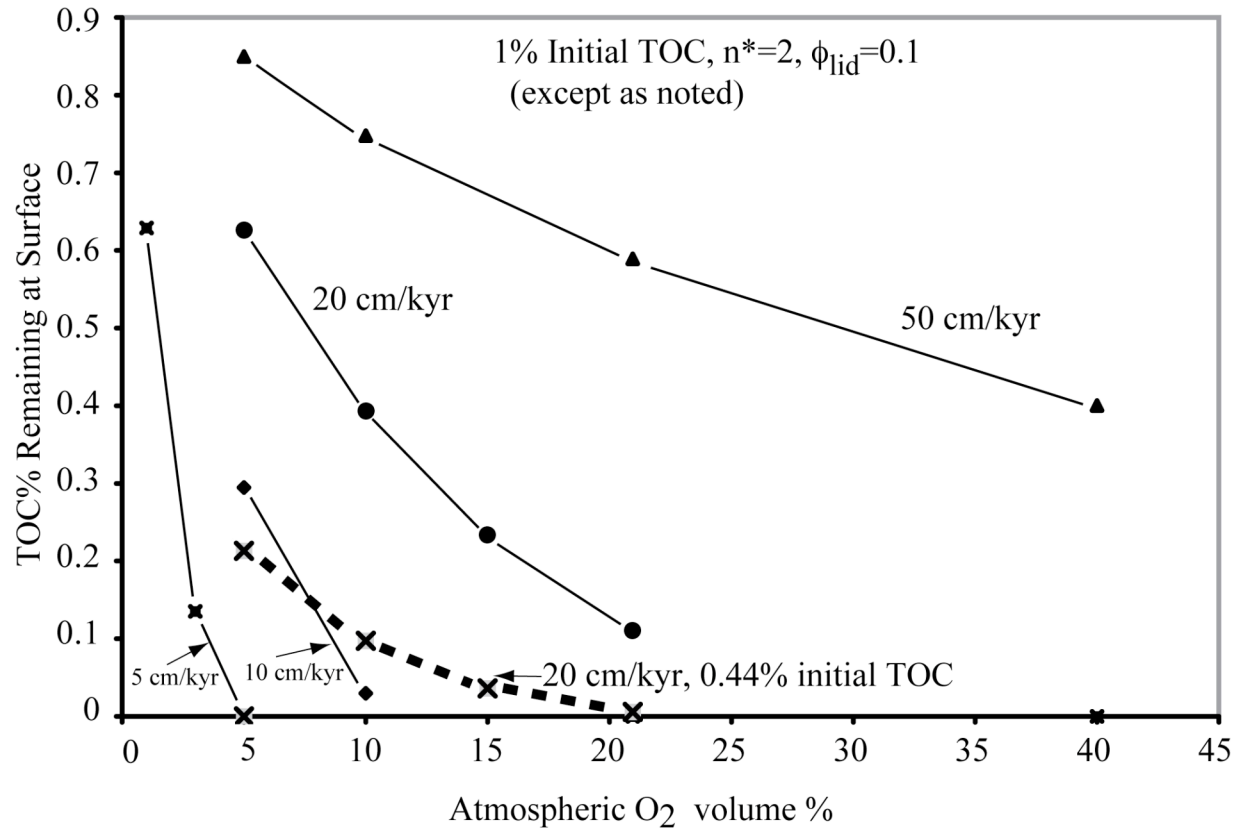Organic matter and pyrite weathering in an eroding black shale

Data / Model comparison
from Bolton, Berner, and Petsch, (2006)

Figure 5. Model results and data for porosity, organic matter as total organic carbon (TOC) and pyrite S. Depth profiles of the field data (A) from our previous study (Wildman and others, 2004). Part A shows the averages of the data at each depth for mass percentages of TOC, total S, and the porosity volume %. (B) Model profiles at steady state. These results used Michaelis-Menten kinetics (from the data of Chang and Berner, 1999) for organic matter (OM) and power law kinetics for pyrite oxidation. This model used 0.45 for air to pore volume ratio, present levels of atmospheric oxygen, a 5cm/kyr erosion rate, initial OM thickness of 10 microns, initial pyrite thickness of 20 microns, 8.3 wt.% TOC, 13.1 wt.% pyrite (about 7.0 wt.% pyrite S) and tortuosity parameter n*=2 (see text). ϕ_{tot} is the total porosity, for which data was not measurable near the surface. (from Bolton, Berner, and Petsch, Am. J. Science, 2006, v. 306, pp. 575-615. to appear)

From Bolton, Berner, and Petsch, (2006)

1% Initial TOC, $n^*=2$, $\phi_{lid}=0.1$
(except as noted)

TOC% Remaining at Surface

20 cm/kyr

50 cm/kyr

5 cm/kyr   10 cm/kyr

20 cm/kyr, 0.44% initial TOC

Atmospheric O_2 volume %

Most OM is consumed before reaching the surface unless erosion rates are high.
This disallows the oxygen level feedback proposed by Lasaga and Ohmoto (2002)

Adapted from Bolton (2006) poster V31B-0592, Fall AGU

Balance of fluxes with front depth as a simple
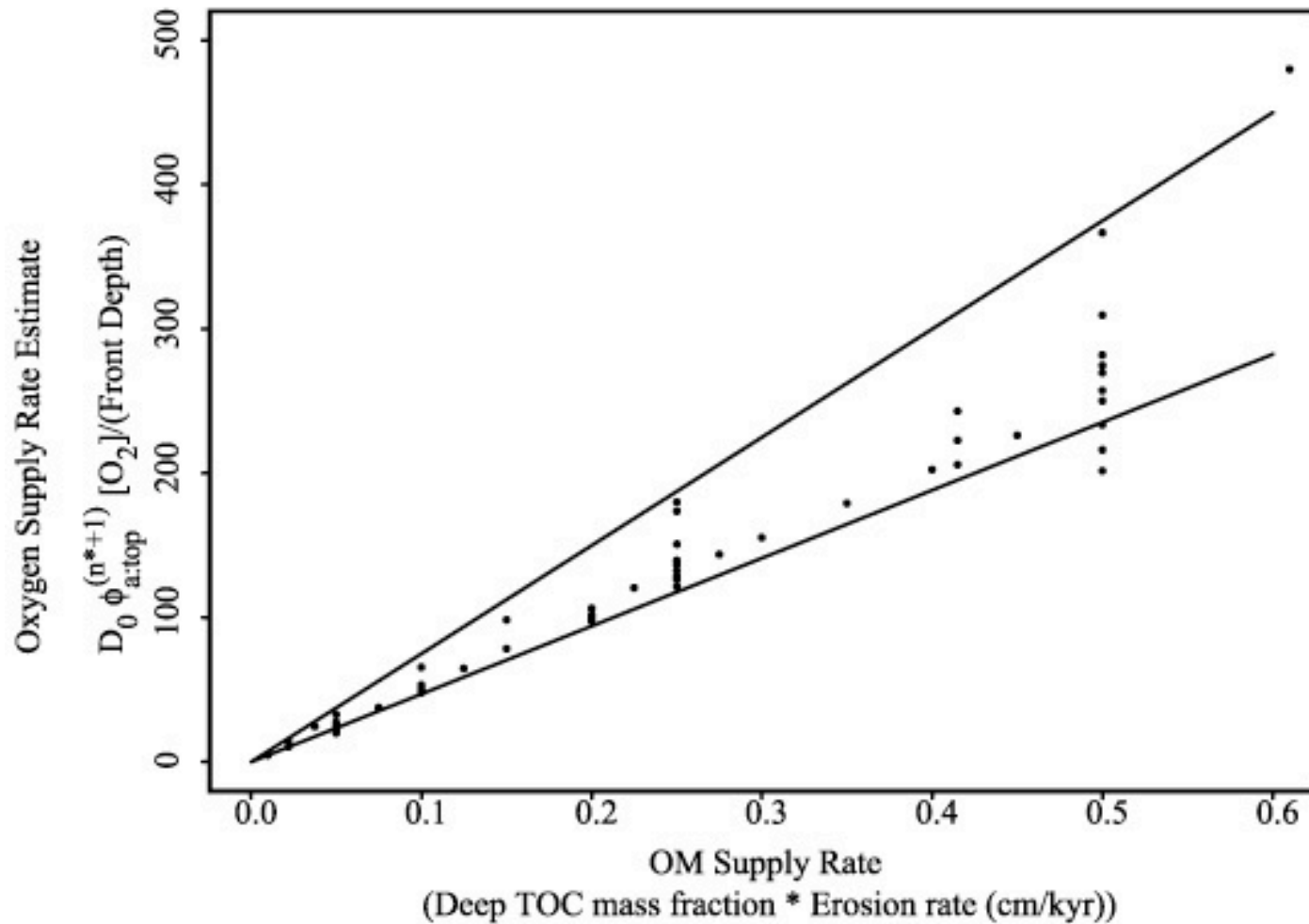scale for Δx of the gradient operator.

Figure 15.

Email edward.bolton@yale.edu

With subject "Code Release" if you are interested in more information. Tell me which of the software items you would be most interested in. I will be distributing more information to those who want to be on the mailing list for this code and documentation release.

Licensing

The code release will be free of charge, but without any implied liability or "goodness of use" guarantees. We will use either the GNU General Public License (Free Software Foundation) or the BSD License (Open Source Initiative).

Adapted from Bolton (2006) poster V31B-0592, Fall AGU

References

• Balashov, V.N., and B.W.D. Yardley, (1998) Modeling metamorphic fluid flow with reaction-compaction-permeability feedbacks, American J. Science, v. 298, 441-470.
• Berman, R.G. (1988) Internally-consistent thermodynamic data for minerals in the system $Na_2O-K_2O-CaO-MgO-FeO-Fe_2O_3-Al_2O_3-SiO_2-TiO_2-H_2O-CO_2$. JPET, v. 29, 445-522.
• Bolton, E. W., Berner, R. A., and Petsch, S. T., (2006) The weathering of sedimentary organic matter as a control on atmospheric O2: II. Theoretical Modeling, to appear: American Journal of Science, October, Vol. 306, pp. 575-615.
• Bolton, E.W., D.M. Rye, J.J. Ague, and A. Luttge, (2004) Modeling contact metamorphism of siliceous dolomite via kinetic control of overall reactions, Water-Rock Interaction, Vol. 1, R.B. Wanty and R.R. Seal II, eds., Proceedings of the 11th International Symposium on Water-Rock Interaction, 27 June -2 July 2004, Saratoga Springs, NY, USA, pp. 269-272.
• Chai, B.H.T., 1975, The kinetics and mass transfer of calcite during hydrothermal recrystallization process, Ph.D. Dissertation, Yale University, New Haven, Connecticut, 203 p.
• Chang, S. & Berner, R.A. 1999. Coal weathering and the geochemical carbon cycle, Geochim. Cosmo. Acta, 63: 3301-3310.
• Christensen, U., and H. Harder (1991) 3--D convection with variable viscosity, Geophys. J. Int., 104, 213--226.
• Eisenstat, S., M. Gursky, M. Schultz, A. Sherman (1977a) Yale sparse matrix package I, The symmetric codes, Report, 112, Dept. Comput. Sci., New Haven, CT.
• Eisenstat, S., M. Gursky, M. Schultz, A. Sherman (1977b) Yale sparse matrix package. II. The nonsymmetric codes, Research Report, 114, Dept. Comput. Sci., New Haven, CT.
• Gleisner, M., Herbert, R. B., and Frogner, P. C., 2004, Microbial pyrite oxidation at various oxygen partial pressures: Geochimica et Cosmochimica Acta, v. 68, no. 11, Supplement S, June 2004, p. A146-A146.

Adapted from Bolton (2006) poster V31B-0592, Fall AGU

References -continued

• Holland, H. D., 2003, Discussion of the article by A. C. Lasaga and H. Ohmoto on "The oxygen geochemical cycle: Dynamics and stability, Geochimica et Cosmochimica Acta, 66, 361-381, 2002": Geochimica et Cosmochimica Acta, v. 67, no. 4, 787-789.

• Kerrick D.M., and Jacobs, G.K. (1981) A modified Redlich-Kwong equation for H_2O-CO_2 mixtures at elevated pressures and temperatures. Am. J. of Science, v. 281, 735-767.

• Lasaga, A. C., and Ohmoto, H., 2002, The oxygen geochemical cycle: Dynamics and stability: Geochimica et Cosmochimica Acta, v. 66, no. 3, 361-381.

• Leonard, B.P., (1984) Third-order upwinding as a rational basis for computational fluid dynamics, in Computational Techniques and Applications: CTAC-83, edited by J. Noye and C. Fletcher, pp. 106-120, Elsevier, New York.

• Luttge, A., E.W. Bolton, and D.M. Rye (2004) A kinetic model of metamorphism: An application to siliceous dolomites, Contributions to Mineralogy and Petrology, DOI: 10.1007/s00410-003-0520-8, Vol. 146, No. 5, January 2004, pp. 546 - 565.

• Ohmoto, H., 2003, Reply to comments by H. D. Holland on "The oxygen geochemical cycle: Dynamics and stability, Geochimica et Cosmochimica Acta, 66, 361-381, 2002", Geochimica et Cosmochimica Acta, v. 67, no. 4, 791-795.

• Smith, E. E., and Shumate, K. S., 1970, Sulfide to sulfate reaction mechanism: A study of the sulfide to sulfate reaction mechanisms as it relates to the formation of acid mine waters: Columbus, Ohio, Ohio State University Research Foundation, report for grant no. 14010 FPS for the Federal Water Pollution Control Administration, Research study #14010-FPS-02/70, U.S. Government Printing Office: 1970 O-384-187.

• White, A.F., and Brantley, S.L., (2003) The effect of time on the weathering of silicate minerals: why do weathering rates differ in the laboratory and field? Chemical Geology, 202, p. 479-506.

• Wildman, R. A., Berner, R. A., Petsch, S. T., Bolton, E. W., Eckert, J.O., Mok, U., and, Evans, J.B., (2004) The weathering of sedimentary organic matter as a control on atmospheric O2: I. Analysis of a black shale, American Journal of Science, Vol. 304, p. 234-249.

• Zhang, S., Paterson, M.S., and Cox, S.F., (1994) Porosity and permeability evolution during hot isostatic pressing of calcite aggregates, J. Geophys. Res., 99, 15741-15760.